

Inflation from Multiple Pseudo-Scalar Fields: PBH Dark Matter and Gravitational Waves

ALIREZA TALEBIAN ¹, SEYED ALI HOSSEINI MANSOORI ² AND HASSAN FIROUZJAH ¹

¹*School of Astronomy, Institute for Research in Fundamental Sciences (IPM), Tehran, Iran, P.O. Box 19395-5531*

²*Faculty of Physics, Shahrood University of Technology, P.O. Box 3619995161 Shahrood, Iran*

ABSTRACT

We study a model of inflation with multiple pseudo-scalar fields coupled to a $U(1)$ gauge field through Chern-Simons interactions. Because of parity violating interactions, one polarization of the gauge field is amplified yielding to enhanced curvature perturbation power spectrum. Inflation proceeds in multiple stages as each pseudo-scalar field rolls towards its minimum yielding to distinct multiple peaks in the curvature perturbations power spectrum at various scales during inflation. The localized peaks in power spectrum generate Primordial Black Holes (PBHs) which can furnish a large fraction of Dark Matter (DM) abundance. In addition, gravitational waves (GWs) with non-trivial spectra are generated which are in sensitivity range of various forthcoming GW observatories.

Keywords: Cosmic inflation, Primordial black hole, Gravitational waves (GWs), GWs observations

1. INTRODUCTION

Inflation is the leading paradigm for early universe cosmology and the mechanism behind the generation of large scale structures. Among the basic predictions of models of inflations are that the primordial perturbations are nearly scale invariant, adiabatic and Gaussian which are well consistent with cosmological observations (Akrami et al. 2020). While the simplest models of inflation are based on a single scalar field, having inflation driven by multiple scalar fields along with other types of fundamental fields in the spectrum is well-motivated in models of high energy physics (Weinberg 2008; Wands 2008; Baumann 2011). In particular, there have been growing interests in the axion models (McAllister et al. 2010; Anber & Sorbo 2010; Barnaby et al. 2011; Barnaby & Peloso 2011; Durrer et al. 2011; Bugaev & Klimai 2014; Linde et al. 2013; Garcia-Bellido et al. 2016; Talebian et al. 2022) to amplify the primordial power spectrum for PBHs formation and to generate detectable GWs signals.

PBHs are distinct from their astrophysical counterparts in several ways. Among all, PBHs could form in the early universe from the collapse upon horizon re-entry of perturbations generated during inflation which may comprise a large fraction of DM energy density (Carr 1975a; Carr et al. 2010; Carr & Kuhnel 2020; Carr et al. 2016; Sasaki et al. 2018). However, PBHs can form through different channels in the early universe as

well (Khlopov 2010; Carr et al. 2021). Remarkably, unlike astrophysical black holes, PBHs can include a vast range of masses. Therefore, the recent observations of GWs from merging binary systems with about 30 times solar mass (Abbott et al. 2016) together with the lack of observational signals of particle DM have renewed the interests in PBHs from inflation (Bird et al. 2016; Clesse & Garcia-Bellido 2017; Sasaki et al. 2016). To produce PBHs from inflation one requires that the amplitude of the primordial curvature perturbation is large enough, at least 10^7 times larger than its CMB value. Over the past a variety of single field models have been studied to provide such enhancement, for a review see (Sasaki et al. 2016; Green & Kavanagh 2021; Byrnes & Cole 2021) and the references therein.

Among multiple-field inflation scenarios N-flation is an interesting example which is based on many axion fields, providing a simple radiatively stable realization of chaotic inflation (Dimopoulos et al. 2008). In this model, the collective contributions of N axion fields yield a long enough period of inflation to solve the flatness and horizon problems. In this picture, inflation is divided to N slow-roll phases where each phase is driven by one axion while others are nearly frozen. Inspired by N-flation model, in this work, we study an inflationary model with multiple pseudo-scalar fields coupled to a $U(1)$ gauge field through Chern-Simons types of interaction. We examine the enhancement of the curvature power spectrum to form PBHs at small scales. We show

that PBHs can be formed abundantly (in the allowed window where PBHs could provide a substantial part of the DM, if not all) without introducing specific features on the inflationary potentials. In addition, tensor perturbations with non-trivial spectrum are generated which may be detected in upcoming GWs experiments.

2. THE MODEL AND BACKGROUND DYNAMICS

We consider N pseudo-scalar fields Φ_a ($a = 1, 2, \dots, N$) driving inflation in N stages. While our starting discussions are general but for specific examples studied below, we consider the cases $N = 2, 3$ specifically. In each stage, only one pseudo-scalar field can slow-roll and then decay, while others remain frozen. The next inflationary stage is driven by the second field before it decays and so on. For this picture to be realized, we need a working hierarchy on the masses of Φ_a , such that the most massive field starts rolling first, then the second most massive field and so on (Yokoyama et al. 2008). For example if the ratio of the mass of Φ_1 to Φ_2 is at the order 10 or so, then we can safely assume that the first period of inflation is driven by Φ_1 . As in single field axion model we demand that all pseudo-scalar fields couple to a $U(1)$ gauge field A_μ through the Chern-Simons interactions (Anber & Sorbo 2006a; Bachlechner et al. 2019) in the following action

$$S = \int d^4x \sqrt{-g} \left[\frac{M_{\text{Pl}}^2}{2} R - \frac{1}{2} \delta^{ab} g^{\mu\nu} \partial_\mu \Phi_a \partial_\nu \Phi_b - V(\Phi_a) - \frac{1}{4} F_{\mu\nu} F^{\mu\nu} - \frac{1}{4} \sum_{a=1}^N \tilde{\alpha}_a \left(\frac{\Phi_a}{M_{\text{Pl}}} \right) F_{\mu\nu} \tilde{F}^{\mu\nu} \right], \quad (1)$$

in which M_{Pl} is the reduced Planck mass, R is the Ricci scalar associated with the spacetime metric $g_{\mu\nu}$. In addition, $\tilde{F}^{\mu\nu} \equiv \epsilon^{\mu\nu\rho\sigma} F_{\rho\sigma}/2$ is the dual of the gauge field strength tensor $F_{\mu\nu} = \nabla_\mu A_\nu - \nabla_\nu A_\mu$. Finally, $\tilde{\alpha}_a$ is a dimensionless parameter controlling the coupling of the a -th pseudo-scalar field to the electromagnetic field (Anber & Sorbo 2006a). To simplify the analysis below, we assume that all $\tilde{\alpha}_a$ have the same sign. This is a technical tuning which simplifies the analysis significantly but it can be relaxed in a more general consideration.

In the presence of coupling $\tilde{\alpha}_a$, the gauge field quanta exhibit tachyonic instability sourced by the rolling pseudo-scalar fields. More precisely, during the a -th stage of inflation, only the field Φ_a rolls slowly. The rolling of this Φ_a amplifies one polarization (e.g. the negative-helicity) of the gauge field, leading to (Anber & Sorbo 2006b)

$$A_k^{(-)} \simeq \frac{e^{\pi\xi - \sqrt{8\xi k/(aH)}}}{\sqrt{2k}} \left(\frac{k}{2\xi aH} \right)^{\frac{1}{4}}; \quad \xi \equiv \sum_{a=1}^N \frac{|\tilde{\alpha}_a \dot{\phi}^a|}{2H}, \quad (2)$$

where k is the comoving Fourier mode of the gauge field, \mathbf{a} and $H \equiv \dot{\mathbf{a}}/\mathbf{a}$ respectively are the scale factor and the Hubble expansion rate during inflation and ϕ_a is the homogeneous part of the pseudo-scalar field Φ_a . The dot denotes the derivative with respect to the cosmic time. The above solution well describes the growth of the mode functions in the interval $(8\xi)^{-1} \lesssim k/(aH) \lesssim 2\xi$ (Barnaby & Peloso 2011). Note also that the other polarization state (here the positive-helicity) is not amplified and can therefore be ignored. The so-called *instability parameter* ξ can be considered nearly constant, as its time variation is subleading in a slow-roll expansion. It is worth mentioning that the gauge quanta (2) not only affect the background dynamics of ϕ_a and the scale factor but also source scalar perturbations via *inverse decay* (Barnaby et al. 2011; Barnaby & Peloso 2011; Barnaby et al. 2012). We assume that $\dot{\phi}_a < 0$ during inflation as in the large field models like (5) so for $\tilde{\alpha}_a > 0$ the negative-helicity is amplified. As mentioned before, we assume that all $\tilde{\alpha}_a$ are positive so only $A_k^{(-)}$ is amplified at each stage of inflation.

Since the gauge field has no background value one can calculate their effects on the background dynamics via mean field approximation method (Linde et al. 2013; Talebian et al. 2022), yielding to

$$3M_{\text{Pl}}^2 H^2 - V - \frac{1}{2} \delta^{ab} \dot{\phi}_a \dot{\phi}_b = \rho_{em} \simeq \frac{\Gamma(7)}{2^{19}\pi^2} \frac{H^4}{\xi^3} e^{2\pi\xi}, \quad (3)$$

$$\ddot{\phi}_a + 3H \dot{\phi}_a + \frac{\partial V}{\partial \phi_a} = \mathbf{J}_a \simeq -\frac{\tilde{\alpha}_a \Gamma(8)}{2^{21}\pi^2} \frac{H^4}{\xi^4} e^{2\pi\xi} \quad (4)$$

Note that the contributions in right hand sides above come respectively from $\rho_{em} \propto \langle E^2 + B^2 \rangle$ and $\mathbf{J}_a \propto \tilde{\alpha}_a \langle \mathbf{E} \cdot \mathbf{B} \rangle$ where the electric and magnetic fields, in the Coulomb-radiation gauge ($A_0 = 0 = \partial_i A^i$), are defined as $E^i \equiv -\mathbf{a}^{-1} \dot{A}^i$ and $B^i \equiv \mathbf{a}^{-2} \epsilon^{ijk} \partial_j A_k$ respectively. The exponential enhancement reflects significant non-perturbative gauge particle production in the regime $\xi \gtrsim 1$ (Anber & Sorbo 2010). To ensure that the tachyonic growth of gauge field fluctuations does not spoil the inflationary dynamics, we demand $H^2/|\dot{\phi}^a| \ll \mathcal{O}(10^2) \xi^{3/2} e^{-\pi\xi}$ at each a -th stage (Barnaby & Peloso 2011; Barnaby et al. 2011; Talebian et al. 2022). From Eq. (4), one finds that the growth of ξ comes to a halt when the back-reaction term becomes large enough. Note that the system experiences a non-linear phase for large coupling, e.g. $\tilde{\alpha} > 20$. This regime is known as the strong back-reaction regime (Caravano et al. 2022). Furthermore, ξ does not experience the oscillatory epoch discussed in (Cheng et al. 2016; Domcke et al. 2020; Caravano et al. 2022; Peloso & Sorbo 2022), because before entering this phase at the end of previous stage, the next rolling field dictates the evolution of ξ .

We work in the regime of negligible back-reaction such that the system never enter this phase and the evolution of ξ can not destroy the inflationary dynamics driven by the pseudo-scalar ϕ_a .

A simple choice for the inflation potential is the chaotic-type potentials ($V = \sum_{a=1}^N m_a^2 \Phi_a^2$) (Dimopoulos et al. 2008; Yokoyama et al. 2008; Anber & Sorbo 2006a) as in N-fflation such that during the a -th stage only the field ϕ_a rolls down towards its potential minimum for some e -folds, oscillating rapidly at the bottom of its potential till its amplitude is effectively died out and the next field starts its rolling. However, the chaotic potentials is rule out by current Planck constraints (Akrami et al. 2020) even in the multi-field configuration (Wenren 2014; Easther & McAllister 2006) due to the large tensor-to-scalar ratio value, r_t . For example, for the two-field and three-field ($N = 2, 3$) axion models with the pure chaotic potentials, our numerical results indicate that $r_t \gtrsim 0.1$ which is in conflict with large scale CMB observations (Akrami et al. 2020). One possible way to avoid this issue is to consider the following simple potential form (Kallosh et al. 2019; Kallosh & Linde 2022a; Braglia et al. 2020a,b; Kallosh & Linde 2022b)

$$V(\Phi^a) = V_0 \frac{\Phi_1^2}{\Phi_1^2 + m_1^2} + \sum_{a=2}^N \frac{1}{2} m_a^2 \Phi_a^2, \quad (5)$$

where V_0 , m_1 , and m_a are constant parameters. In two-field case, this potential represents the well-known dilaton-axion inflation (Linde et al. 2018; Kallosh & Linde 2022a). We arrange that on CMB scales the first pseudo-scalar field (the dilaton field) drive inflation while the remaining pseudo-scalar fields ($N \geq 2$) with the standard chaotic type potential (now specifically called axionic fields) drive the rest of inflation. Recently, in (Braglia et al. 2020a,b; Kallosh & Linde 2022b) the authors have shown that PBHs and GWs might be generated by considering a non-flat field space with the negative curvature in the absence of Chern-Simons coupling. In comparison, here we work with the flat field space while the instabilities induced from the Chern-Simons coupling are responsible for amplification of power spectra. Also note that instead of potential (5) one may consider different examples as well. We only need to assume the first stage of inflation is driven with a potential different than simple chaotic potential such that on CMB scales the value of r_t is small enough.

After presenting the general setup, in the following we consider two specific models: dilaton-axion (model I) and dilaton-axion-axion (model II). Table 1 presents the initial conditions and model parameters. The parameters are fixed to produce the correct COBE normalization at the CMB pivot scale

$k_{\text{CMB}} = 0.05 \text{ Mpc}^{-1}$ (Akrami et al. 2020). In addition, the parameter $\tilde{\alpha}_1$ for model I and $\tilde{\alpha}_2$ for model II have adopted the largest possible values consistent with the PBH bound (Garcia-Bellido et al. 2016) while $\tilde{\alpha}_1$ for model II has adopted the largest possible values consistent with the NANOGrav 11yrs data release (Arzoumanian et al. 2018).

As shown in Figs. 1 and 2, the background experiences several inflationary phases in both models. The first inflationary phase is driven by dilaton Φ_1 while the other fields remain frozen. After Φ_1 has reached to its minimum and its energy is died out after a few rapid oscillations the axion fields drive the next inflationary phase each in turn. The evolution of the Hubble parameter is also presented in Figs. 1 and 2 in accord with multiple inflationary phases. The numerical values of $\{N_{\text{end}}, r_t, n_s\}$ for the total number of e -folding, the tensor-to-scalar ratio, and the spectral index on CMB scales are $\{61.1, 0.014, 0.961\}$ for model I and $\{62.5, 0.032, 0.935\}$ for model II which are in close agreement with analytic results (Kallosh & Linde 2022a).

As mentioned earlier, we must ensure that the tachyonic growth of gauge field fluctuations does not modify the slow-roll inflationary dynamics. To do this, let us define the following back-reaction parameters

$$R_a \equiv \left| \frac{J_a}{3H\dot{\phi}_0} \right| \ll 1; \quad \Omega_{\text{em}} \equiv \frac{\rho_{\text{em}}}{3M_{\text{Pl}}^2 H^2} \ll 1, \quad (6)$$

which measure the back-reaction effects on the dynamics of rolling fields and the total energy density, respectively. As shown in Fig. 3, these dimensionless parameters are small so the evolution of ξ does not destroy the inflationary dynamics driven by the pseudo-scalars for the parameter range which we work.

Table 1. Model parameters ($\tilde{\alpha}_a, m_a$) and initial conditions for pseudo-scalar fields, ϕ_*^a with $V_0 = 500m_2^2 M_{\text{Pl}}^2$ and $m_1 = \sqrt{6}M_{\text{Pl}}$ for both models and define the dimensionless parameters $\tilde{m}_a \equiv 10^5 m_a/M_{\text{Pl}}$ and $\tilde{\phi}_*^a \equiv \phi_*^a/M_{\text{Pl}}$. The couplings to gauge fields $\tilde{\alpha}$ are chosen as large as allowed by the PHB bounds (Garcia-Bellido et al. 2016) and NANOGrav 11yrs data sets (Arzoumanian et al. 2018)

Model	$(\tilde{\alpha}_1, \tilde{\phi}_*^1)$	$(\tilde{\alpha}_2, \tilde{\phi}_*^2, \tilde{m}_2)$	$(\tilde{\alpha}_3, \tilde{\phi}_*^3, \tilde{m}_3)$
I	(10.2, 5.8)	(5, 10.5, 0.125)	-
II	(8.7, 5)	(13.2, 8.0, 2)	(5, 10, 0.02)

3. CURVATURE PERTURBATIONS AND PBH FORMATION

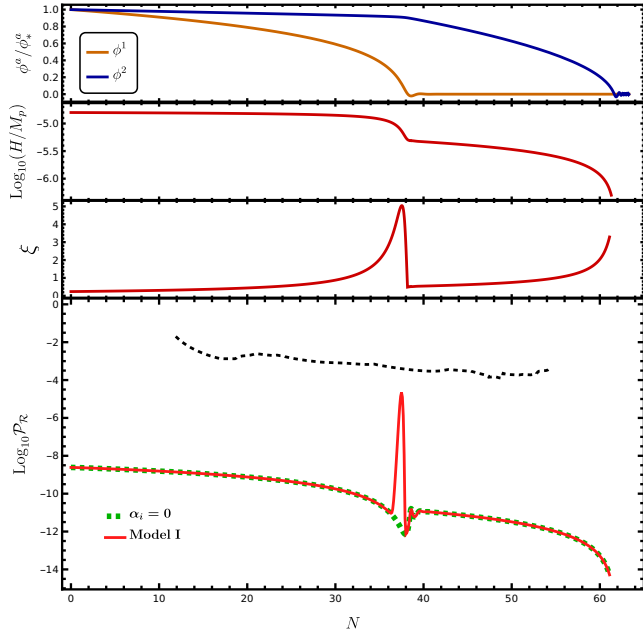


Figure 1. Evolution of the scalar fields, Hubble rate, instability parameter, and $\mathcal{P}_{\mathcal{R}}$ for the model I with two pseudo-scalars (one dilaton and one axion). The black dashed curve presents the PBH bound (Garcia-Bellido et al. 2016). A rise in ξ yields to a localized peak in $\mathcal{P}_{\mathcal{R}}$. Note that the green dashed curve shows that the power can not be enhanced when $\tilde{\alpha}_i = 0$.

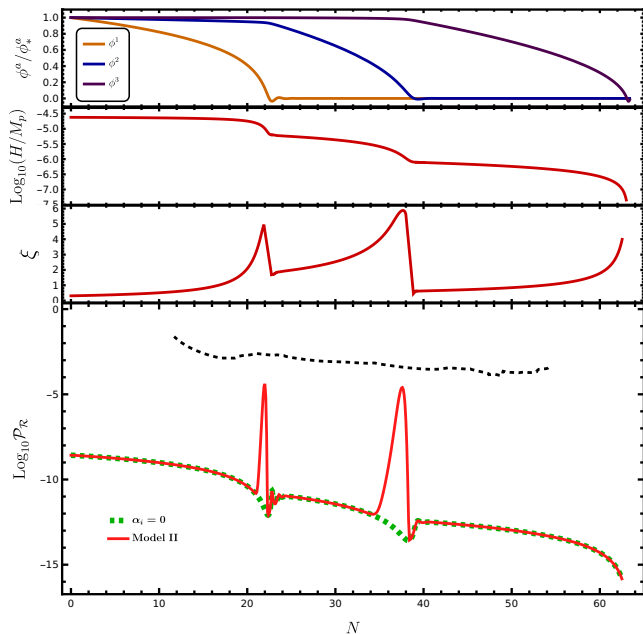


Figure 2. The same as in Fig. 1 but for the model II. Since we have three pseudo-scalars (one dilaton and two axions) there are two peaks in evolution of ξ yielding to two localized peaks in $\mathcal{P}_{\mathcal{R}}$.

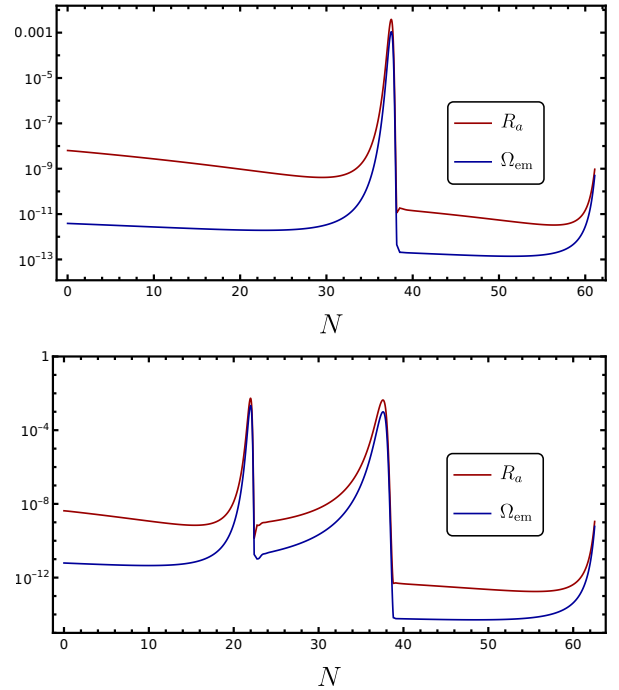


Figure 3. Evolution of the back-reaction parameters for model I (top) and model II (below). We see that both of these parameters are small and the back-reactions effects are negligible.

Now we study the evolution of fluctuations in our setup. Because of the coupling between the scalar fields and the gauge field, there will be source terms in the equation of motion of the scalar field fluctuations. The scalar field Φ^b can be decomposed into the background part ϕ^b and its canonical perturbation \hat{Q}^b as $\Phi^b = \phi^b + \mathbf{a}\hat{Q}^b$. In the spatially flat gauge, the equation of motion for the modes \hat{Q}_k^a in momentum space reads (Dimastrogiovanni et al. 2018; Linde et al. 2013; Özsoy 2018)

$$\left(\partial_\tau^2 + k^2 - \frac{\mathbf{a}''}{\mathbf{a}}\right)\hat{Q}_k^a(\tau) + \mathbf{a}^2\left(\frac{\partial^2 V}{\partial\phi^a\partial\phi^b}\right)\hat{Q}_k^b(\tau) = \frac{\tilde{\alpha}^a\mathbf{a}^3}{f}\int\frac{d^3k}{(2\pi)^{3/2}}e^{-i\mathbf{k}\cdot\mathbf{x}}\vec{E}\cdot\vec{B}, \quad (7)$$

where τ is the conformal time, $d\tau \equiv \mathbf{a}(t)dt$. The solution for \hat{Q}^a can be separated into two uncorrelated parts $\hat{Q}_a = \hat{Q}_a^{(v)} + \hat{Q}_a^{(s)}$ where $\hat{Q}_a^{(v)}$ represents the solution to the homogeneous part of Eq. (7) which reduces to Bunch-Davies vacuum on small scales, whereas $\hat{Q}_a^{(s)}$ is the particular solution obtained by the Green function (Barnaby et al. 2011). Also, since there is no interaction between the fields, the equations for \hat{Q}^a are decoupled. Finally, the power spectrum of curvature perturbations, which is defined as $\mathcal{R}_k = \sum_a (H/\mathbf{a}\dot{\phi}^a)\hat{Q}_k^i$ at horizon crossing time, N_k , becomes (Barnaby & Peloso 2011;

Barnaby et al. 2011)

$$\mathcal{P}_{\mathcal{R}}(k) \simeq \frac{H^2}{8\pi^2 M_{\text{Pl}}^2 \epsilon_H} \left(1 + \frac{H^2}{8\pi^2 M_{\text{Pl}}^2 \epsilon_H} f_2(\xi) e^{4\pi\xi} \right), \quad (8)$$

where ϵ_H is the first slow-roll parameter and the dimensionless function $f_2(\xi)$ can be estimated for large ξ as $10^{-5}/\xi^6$ (Barnaby et al. 2011). The first term in Eq. (8) stands for the standard vacuum contribution to the power spectrum (Yokoyama et al. 2008; Baumann 2011).

The curvature perturbations power spectrum for the models in Table 1 are illustrated in Fig. 1 and 2. As can be seen, a rise in ξ amplifies the scalar power spectrum for the mode that leaves the Hubble radius at the transition time between the two stages. The location of a -th peak, N_a (number of e-fold since the start of inflation), is given by the initial condition ϕ_*^a , while the amplitude of $\mathcal{P}_{\mathcal{R}}(k)$ is controlled by $\tilde{\alpha}_a$. Interestingly, for values of $\tilde{\alpha}_a$ considered in Table 1, the enhancement in the power spectrum is large enough to seed PBH formation due to the gravitational collapse of large density fluctuations after horizon re-entry during radiation-dominated era (Sasaki et al. 2018).

After PBH production, the next step is to determine the fraction of PBH abundance in dark matter density at the present epoch. It is roughly given by (Sasaki et al. 2018)

$$f_{\text{PBH}}(M_a) \simeq 2.7 \times 10^8 \left(\frac{M_{\odot}}{M_a} \right)^{\frac{1}{2}} \beta(M_a), \quad (9)$$

where the mass corresponding to a -th peak, M_a , can be estimated by the following relation as we assume an instant reheating at the end of inflation (Garcia-Bellido et al. 2016).

$$\frac{M_a}{M_{\odot}} \simeq 10^{-13} \left(\frac{10^{-6} M_{\text{Pl}} H_{\text{end}}}{H_a^2} \right) e^{2(N_{\text{end}} - N_a - 22.25)}, \quad (10)$$

where M_{\odot} is the solar mass and H_{end} and H_a are the Hubble rates at N_{end} and N_a , respectively. Moreover, the β is the mass fraction of PBHs at formation.

In the Press-Schechter formalism (Press & Schechter 1974), β is defined as the probability that the Gaussian comoving curvature perturbation \mathcal{R} (or equivalently the density contrast δ) is greater than a certain threshold value \mathcal{R}_c (or δ_c) for PBH formation (Press & Schechter 1974; Lyth 2012; Byrnes et al. 2012; Garcia-Bellido et al. 2016). Moreover, one can also compute β by using the peak theory formalism where the primordial over density condition is expressed in terms of the peak value of a fluctuation mode (Young et al. 2014; Musco 2019; Yoo et al. 2018), in contrast to the average value utilized in Press-Schechter theory. In addition, in the peak theory formalism, the PBH formation probability is highly

sensitive to the change in the tail of the fluctuation distribution.

The threshold for PBHs at the cosmological horizon crossing has been widely computed in the literature by making use of a linear extrapolation from the superhorizon regime. However, since the non-linear relation between the density contrast and the curvature perturbation is neglected it does not yield to the right amplitude of the perturbation at the cosmological horizon crossing (Biagetti et al. 2021; Musco 2019).

Taking into account this non-linear effects, the mass fraction is defined as (Biagetti et al. 2021)

$$\beta \equiv \int_{\delta_{l,c}}^{4/3} d\delta_l \kappa \left(\delta_l - \frac{3}{8} \delta_l^2 - \delta_c \right)^{\tilde{\gamma}} f_{\delta_l}(\delta_l) \quad (11)$$

where the probability distribution $f_{\delta_l}(\delta_l)$ is given by (A7), $\kappa = 3.3$, and $\tilde{\gamma} = 0.36$ for the collapse at the radiation-dominated epoch. Moreover, the field δ_l depends on the threshold density contrast through the following expression (see App. A for more details).

$$\delta_{l,c} = \frac{4}{3} \left(1 - \sqrt{1 - \frac{3}{2} \delta_c} \right) \quad (12)$$

in which one can take $\delta_c \simeq 0.59$ for a monochromatic curvature perturbation power spectrum (Musco 2019; Musco et al. 2021a).

In Fig. 4, we have depicted f_{PBH} for the models introduced in Table 1. As illustrated, the formed PBHs can furnish a large fraction of total DM abundance. In particular, for model I and II, we obtain $f_{\text{PBH}} \simeq 1$ corresponding to $M_{\text{PBH}} \sim 10^{-14} M_{\odot}$ and $M_{\text{PBH}} \sim 10^{-12} M_{\odot}$, respectively. Additionally, as illustrated in Fig. 2, because the first peak in the scalar power spectrum for model II is not amplified large enough, its corresponding PBH mass, i.e. $M_{\text{PBH}} \sim M_{\odot}$ can not contribute significantly to the dark matter density in the universe today. However, in the case with $\tilde{\alpha}_1 = 8.9$ and the other initial conditions like model II, one obtains $f_{\text{PBH}} \simeq \mathcal{O}(0.1)$ for almost the same PBH mass. In spite of this fact, such a model conflicts with the recent observational constraint on the GWs determined by the NANOGrav 11yrs data release (Arzoumanian et al. 2018).

4. PRIMORDIAL AND INDUCED GWS

In addition to the quantum vacuum fluctuations of metric during inflation, there are two distinct populations of stochastic GWs in our inflationary scenario. The first contribution is related to the GWs generated from the amplified gauge fields during inflation (Barnaby & Peloso 2011; Sorbo 2011; Namba et al. 2016; Özsoy 2021;

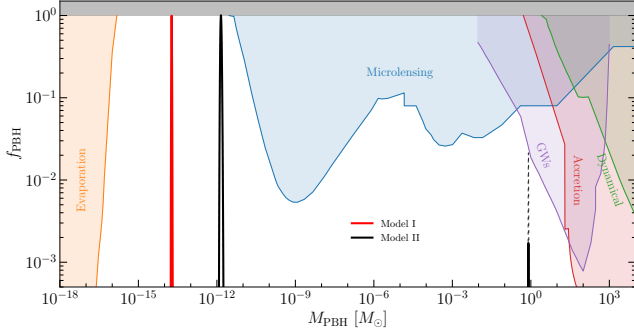


Figure 4. Fraction f_{PBH} as a function of the mass of the formed PBHs in unit of solar mass for models in Table. 1. The observational constraints are taken from Refs. (Green & Kavanagh 2021; Kavanagh 2019; Carr et al. 2021). The black dashed narrow band mass functions, corresponding to $M_{\text{PBH}} \simeq 0.8M_{\odot}$ with $f_{\text{PBH}} \simeq \mathcal{O}(0.1)$ for the case with $\tilde{\alpha}_1 = 8.9$.

Özsoy & Lalak 2021). The second contribution is the so-called *induced* GWs originating from the enhanced second order scalar fluctuations (Tomita 1967; Matarrese et al. 1993, 1994, 1998; Ananda et al. 2007; Baumann et al. 2007; Espinosa et al. 2018; Kohri & Terada 2018; Domènech 2021).

Due to the parity-violating nature of the system, the right and left helicities of tensor modes have different amplitudes (Sorbo 2011). The equation of motion for two canonical tensor helicity \hat{h}^{λ} is given by

$$\left(\partial_{\tau}^2 + k^2 - \frac{2}{\tau^2}\right)\hat{h}_k^{\lambda}(\tau) = \frac{-\mathbf{a}^3}{M_{\text{Pl}}} \Pi_{ij}^{\lambda}(\mathbf{k}) \times \int \frac{d^3k}{(2\pi)^{3/2}} e^{-i\mathbf{k}\cdot\mathbf{x}} [E_i E_j + B_i B_j], \quad (13)$$

where Π_{ij}^{λ} is the transverse traceless projector (Sorbo 2011). Similar to scalar fluctuations, we decompose \hat{h}^{λ} into a vacuum mode, $\hat{h}_{\lambda}^{(\text{v})}$, and the sourced mode, $\hat{h}_{\lambda}^{(\text{s})}$. Adding up these two contributions, one finds the tensor power spectrum for each polarizations mode to be (Sorbo 2011)

$$\mathcal{P}_{\lambda}^{(\text{p})}(k) \simeq \frac{H^2}{\pi^2 M_{\text{Pl}}^2} \left(1 + \frac{2H^2}{M_{\text{Pl}}^2} f_{\lambda}(\xi) e^{4\pi\xi}\right), \quad (14)$$

where the superscript (p) stands for the primordial contribution in which the first term represents the contribution from vacuum fluctuations. Moreover, the dimensionless function $f_{\lambda}(\xi)$ at large ξ for the right and left helicities are approximately $10^{-7}/\xi^6$ and $10^{-9}/\xi^6$, respectively (Sorbo 2011). Correspondingly, the main contribution to the primordial tensor power spectrum, $\mathcal{P}_h^{(\text{p})} = \sum_{\lambda} \mathcal{P}_{\lambda}^{(\text{p})}$, comes from the right helicity GW modes (Sorbo 2011; Barnaby et al. 2012).

As stated earlier, the GWs can be induced from the amplified curvature perturbations in Eq. (8) (Zhou et al.

2020; Domènech et al. 2020; Pi & Sasaki 2020; Cai et al. 2019b; Özsoy & Lalak 2021). Indeed, the large second order scalar fluctuations on small scales induce tensor perturbations after the horizon re-entry during radiation-dominated era. With regard to the population of GWs discussed above, one deals with multiple integrals of the following form (Kohri & Terada 2018)

$$\mathcal{P}_h^{(\text{ind})} \sim \int dk \int dk' \left[\int f(k, k', t) dt \right]^2 \mathcal{P}_{\mathcal{R}}(k) \mathcal{P}_{\mathcal{R}}(k') \quad (15)$$

where $f(k, k', t)$ is an oscillating function and t describes the time when the GW is sourced from the scalar modes (Kohri & Terada 2018; Cai et al. 2019a; Acquaviva et al. 2003; Inomata et al. 2017; Domènech 2021). Finally, the total present-day energy density of GWs is given by (Özsoy & Lalak 2021; Baumann et al. 2007; Espinosa et al. 2018)

$$\Omega_{\text{GW}}(k) = \Omega_{\text{GW}}^{(\text{p})}(k) + \Omega_{\text{GW}}^{(\text{ind})}(k), \quad (16)$$

in which $\Omega_{\text{GW}}^{(\text{p})}(k)$ and $\Omega_{\text{GW}}^{(\text{ind})}(k)$ represent the fraction energy density of primordial GWs induced by the tachyonic gauge field mode and the induced GWs from the second order scalar perturbations respectively.

In Figs. 5 and 6, we have plotted the quantity $\Omega_{\text{GW}} h^2$ (light blue curve) which is the sum of $\Omega_{\text{GW}}^{(\text{p})} h^2$ (green dashed curve), and $\Omega_{\text{GW}}^{(\text{ind})} h^2$ (red dotted curve) against the frequency with $h^2 = 0.49$ together with the sensitivity of the various forthcoming GW experiments *e.g.* the LISA (Bartolo et al. 2016), BBO (Crowder & Cornish 2005; Corbin & Cornish 2006; Baker et al. 2019), SKA (Carilli & Rawlings 2004; Janssen et al. 2015; Weltman et al. 2020), and PPTA (Manchester et al. 2013; Shannon et al. 2015). As can be seen, the summit of the total GW curves are related to $\Omega_{\text{GW}}^{(\text{p})} h^2$, while $\Omega_{\text{GW}}^{(\text{ind})} h^2$ constitutes a sub-dominant portion of the total GW signal around the biggest peak. In addition, the oscillations in the curves originate from convolution integrals in Eq. (15).

Clearly, for the models I, $\Omega_{\text{GW}} h^2$ falls within the sensitivity of the BBO and peaks well inside the range of detectability of LISA. Remarkably, for the model II, we observe that the double rises in GWs are detectable by LISA and SKA. A similar feature has been observed in (Bhaumik et al. 2022) as a signal of a non-thermal baryogenesis from evaporating PBHs.

On the other hand, the current severe constraint on stochastic GW background in nHz regime, *i.e.* NANOGrav 11yrs (Arzoumanian et al. 2018) can put restrictions on the parameters of our model. We observe from Fig. 6 that the first peak of $\Omega_{\text{GW}} h^2$ for model II with $\tilde{\alpha}_1 = 8.7$ is located at SKA scales by respect to

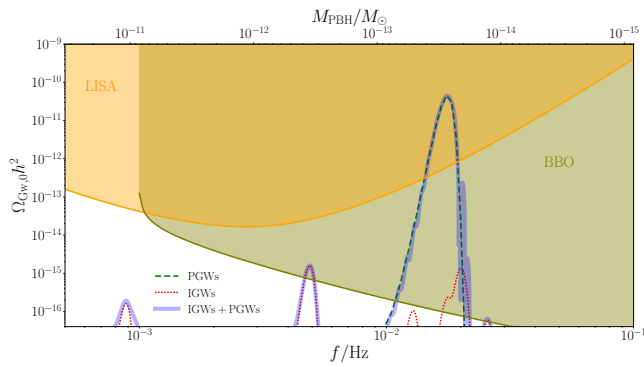


Figure 5. The energy density of the GWs for model I with respect to frequency. The contributions of primordial (polarized) and induced GWs are plotted separately as well. The shadowed regions represent the sensitivity curves of various GW detectors (Schmitz 2021, 2020). The largest peak of the curve is due to primordial polarized GWS given in (14) while the oscillations in the curve originate from convolution integrals in Eq. (15).

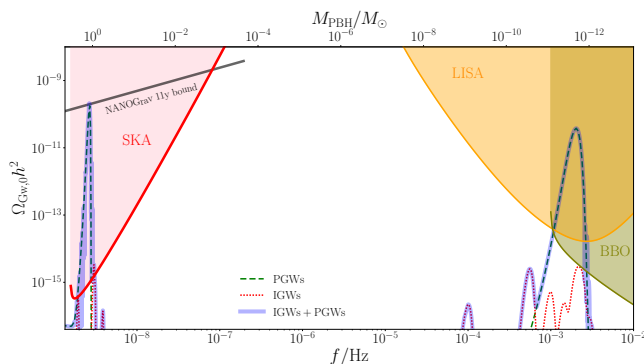


Figure 6. The same as Fig. 5 but for model II. Note that the model II with two rolling axions yields to two separated sets of curves. The black solid line represent the observational limits imposed by the NANOGrav 11yrs data release (Arzoumanian et al. 2018).

the NANOGrav 11yrs bound. However, for the model with $\tilde{\alpha}_1 = 8.9$, the result clashes with the NANOGrav 11yrs constraint. Generally, the both observational data of PBH limits and GWs should be considered together to limit the parameter space of our model.

As a final remark, the sign of $\tilde{\alpha}_a$ determines which polarization of the gauge field is amplified and hence we have considered a simple setup where only one polarization is amplified all the time. Nevertheless, when we switch the signs of $\tilde{\alpha}_a$, then the other polarization gets amplified as well and we must perform the mode analy-

sis more carefully. Moreover, since the peaks in the GW spectrum are so separated, one can observe only one at a time, so the sign of the chirality of the other, non observable ones (at frequencies that are too high/too low) will not matter. We leave a comprehensive analysis on this general situation for a future work.

5. SUMMARY AND DISCUSSIONS

We have studied a model of inflation with multiple pseudo-scalar fields coupled to a gauge field via the Chern-Simons type interactions. There are multiple stages of inflation driven by each scalar field. To evade the constraint on tensor-to-scalar ratio, we have considered a setup where the first stage is driven by a dilaton field while the remaining stages of inflation below CMB scales are driven with multiple axionic fields with the standard chaotic type potentials. However, our setup can be extended to more complicated potentials, such as α -attractor model (Kallos & Linde 2022a). The enhanced power spectrum from the gauge field instability can generate PBHs with various masses which can furnish a large fraction of total DM while satisfying the bounds on PBHs formation (Garcia-Bellido et al. 2016). In addition, GWs can be generated both from second order scalar perturbations as well as from the tachyonic gauge field perturbations with distinct features on the location of the peaks and their oscillatory behaviours. These signals are within the detection range of the future GW observatories. There are a number of directions in which the current investigations can be extended. These include investigating the non-Gaussianity of the perturbations (D’Amico et al. 2022) and its effects on the induced GWs (Adshead et al. 2021; D’Amico et al. 2021) and the PBHs formation (Biagetti et al. 2021).

- 1 This work is dedicated to the memory of Prof. Mo-
- 2 hammad Reza Setare (1974-2022). We are grateful to
- 3 Lorenzo Sorbo for useful comments on the draft. We
- 4 acknowledge the partial support from the “Saramadan”
- 5 federation of Iran. A. T. would like to thank Yukawa
- 6 Institute for Theoretical Physics (YITP) for their kind
- 7 hospitality during the development of this work. We
- 8 would like to thank the anonymous referee for the in-
- 9 sightful comments and suggestions which have improved
- 10 the quality of the paper.

APPENDIX

A. PDF OF THE DENSITY CONTRAST

The main aim of this appendix is to derive the probability distribution function (PDF) for the smoothed density contrast and hence compute the mass fraction β . By following the same methodology proposed in (Biagetti et al. 2021), we first consider the smoothed density contrast, δ_m , as (Biagetti et al. 2021; Musco 2019; Young et al. 2019)

$$\delta_m = \delta_l - \frac{3}{8}\delta_l^2; \quad \delta_l \equiv -\frac{4}{3}r_m\mathcal{R}'(r_m), \quad (\text{A1})$$

where the prime here denotes the derivative with respect to the radial coordinate r_m which indicates the location of the maximum of the compaction function. More importantly, the relation (A1) shows non-linear relation between the smooth density contrast and spatial derivative of the curvature perturbation¹. Then, thanks to the conservation of the probability, we compute the PDF of the auxiliary field δ_l , indicates by f_{δ_l} , in order to calculate the mass fraction (11).

It is worthwhile noting that, in our case of study, sourced scalar fluctuations $\hat{Q}_a^{(s)}$ originate from the convolution of two Gaussian gauge fields and hence the PDF of curvature perturbation obeys a χ^2 statistics (Linde et al. 2013). Therefore, we can consider (Linde et al. 2013)

$$\mathcal{R} = g^2 - \langle g^2 \rangle \quad (\text{A2})$$

where g stands for the Gaussian distributed field² whose PDF is given by

$$f_g(x) = \frac{1}{\sqrt{2\pi}\sigma_g} \exp\left(-\frac{x^2}{2\sigma_g^2}\right) \quad (\text{A3})$$

in which $\sigma_g^2 \equiv \langle g^2 \rangle$ is the variance. Having the above PDF allows us to find $\langle g^4 \rangle = 3\sigma_g^4$ and hence $\sigma_{\mathcal{R}}^2 \equiv \langle \mathcal{R}^2 \rangle = 2\sigma_g^4$. For simplicity we can consider the power spectra of curvature perturbations shown in Fig. 1 as a monochromatic spectra $\mathcal{P}_{\mathcal{R}}(k) \simeq \mathcal{P}_* k_* \delta_D(k - k_*)$ (where δ_D is the Dirac Delta function) peaked at a momentum scale k_* such that $r_m k_* \simeq 2.74$ (Musco 2019). Therefore, we have

$$\sigma_{\mathcal{R}}^2 \equiv \int d \ln k \mathcal{P}_{\mathcal{R}}(k) \simeq \mathcal{P}_*. \quad (\text{A4})$$

By taking into account the above result, one can relate the variance of Gaussian field g to the amplitude of peak of the curvature perturbation, namely

$$\sigma_g \simeq (\mathcal{P}_*/2)^{1/4}. \quad (\text{A5})$$

In addition, because $\langle g^2 \rangle$ is independent of r_m , one obtains

$$\delta_l = -\frac{8}{3}r_m g g'. \quad (\text{A6})$$

Let us now consider the two uncorrelated fields g and g' which are both Gaussian random fields with the zero mean value. The variance of g' is denoted as $\sigma_{g'} = k_* \sigma_g$. According to the conservation of the probability, the PDF of the density contrast is simply given by

$$\begin{aligned} f_{\delta_l}(\delta_l) &= \int dg dg' \delta_D\left(\delta_l + \frac{8}{3}r_m g g'\right) f_g(g) f_{g'}(g') \\ &= \frac{3}{8r_m} \int dg \frac{f_g(g)}{|g|} f_{g'}\left(\frac{-3\delta_l}{8gr_m}\right) \\ &= \alpha K_0(\alpha |\delta_l|), \end{aligned} \quad (\text{A7})$$

¹ Due to the dependence of the field δ_l on the derivative of the comoving curvature perturbation, one can always add or subtract to the comoving curvature perturbation a constant by a coordinate transformation on superhorizon scales and this may not affect on any physical result.

² The stochastic properties of the gauge field A are close to those in a free theory, namely it has Gaussian perturbations around $\langle A \rangle = 0$.

where $K_n(x)$ is the modified Bessel function of the second kind and

$$\alpha \equiv \frac{3}{8\pi r_m \sigma_g \sigma_{g'}} = \frac{3\sqrt{2}}{8\pi k_* r_m \sqrt{\mathcal{P}_*}} \quad (\text{A8})$$

Through the use of PDF (A7), we are able to compute the PBH mass fraction in Eq. (11) and then estimate the fractional abundance of PBHs at the present epoch via Eq. (9).

Finally, it is worth emphasizing the importance of the nonlinear effects of curvature perturbation, as given in Eq. (A1), for calculating f_{PBH} in our setup. To do so, we consider the conventional method for estimation the mass fraction β . The method is based on the relation

$$\beta \sim \gamma \int_{\mathcal{R}_c}^{\infty} d\mathcal{R} f_{\mathcal{R}}(\mathcal{R}) \quad (\text{A9})$$

where $\mathcal{R}_c \simeq 1$ ³ is the threshold value and $f_{\mathcal{R}}$ is the PDF of the curvature perturbations and the value of the constant of proportionality $\gamma \simeq 0.2$ is proposed in (Carr 1975b; Sasaki et al. 2018). In our case of study, sourced scalar fluctuations $\hat{Q}_a^{(s)}$ originate from the convolution of two Gaussian gauge fields and hence the PDF of curvature perturbation obeys a χ^2 statistics (Linde et al. 2013). Consequently, the fraction β is related to power spectrum of curvature perturbation by (Garcia-Bellido et al. 2016)

$$\beta(N_a) \simeq \text{Erfc} \left(\sqrt{\frac{1}{2} + \frac{\mathcal{R}_c}{\sqrt{2\mathcal{P}_{\mathcal{R}}(N_a)}}} \right) \quad (\text{A10})$$

in which $\text{Erfc}(x) \equiv 1 - \text{Erf}(x)$ is the complementary error function. Using (A10) for for the mass fraction in (9), the maximum value obtained for Table. 1 corresponds to model I with $f_{\text{PBH}} \sim \mathcal{O}(10^{-91})$! This estimate shows that the nonlinear effects of the curvature perturbation play a significant role in generating PBH in this class of models.

REFERENCES

- Abbott, B. P., et al. 2016, Phys. Rev. Lett., 116, 061102, doi: [10.1103/PhysRevLett.116.061102](https://doi.org/10.1103/PhysRevLett.116.061102)
- Acquaviva, V., Bartolo, N., Matarrese, S., & Riotto, A. 2003, Nucl. Phys. B, 667, 119, doi: [10.1016/S0550-3213\(03\)00550-9](https://doi.org/10.1016/S0550-3213(03)00550-9)
- Adshead, P., Lozanov, K. D., & Weiner, Z. J. 2021, JCAP, 10, 080, doi: [10.1088/1475-7516/2021/10/080](https://doi.org/10.1088/1475-7516/2021/10/080)
- Akrami, Y., et al. 2020, Astron. Astrophys., 641, A10, doi: [10.1051/0004-6361/201833887](https://doi.org/10.1051/0004-6361/201833887)
- Ananda, K. N., Clarkson, C., & Wands, D. 2007, Phys. Rev. D, 75, 123518, doi: [10.1103/PhysRevD.75.123518](https://doi.org/10.1103/PhysRevD.75.123518)
- Anber, M. M., & Sorbo, L. 2006a, Journal of Cosmology and Astroparticle Physics, 2006, 018
- . 2006b, JCAP, 10, 018, doi: [10.1088/1475-7516/2006/10/018](https://doi.org/10.1088/1475-7516/2006/10/018)
- . 2010, Phys. Rev. D, 81, 043534, doi: [10.1103/PhysRevD.81.043534](https://doi.org/10.1103/PhysRevD.81.043534)
- Arzoumanian, Z., et al. 2018, Astrophys. J., 859, 47, doi: [10.3847/1538-4357/aabd3b](https://doi.org/10.3847/1538-4357/aabd3b)
- Bachlechner, T. C., Eckerle, K., Janssen, O., & Kleban, M. 2019. <https://arxiv.org/abs/1902.05952>
- Baker, J., et al. 2019. <https://arxiv.org/abs/1907.11305>
- Barnaby, N., Namba, R., & Peloso, M. 2011, JCAP, 04, 009, doi: [10.1088/1475-7516/2011/04/009](https://doi.org/10.1088/1475-7516/2011/04/009)
- Barnaby, N., Pajer, E., & Peloso, M. 2012, Phys. Rev. D, 85, 023525, doi: [10.1103/PhysRevD.85.023525](https://doi.org/10.1103/PhysRevD.85.023525)
- Barnaby, N., & Peloso, M. 2011, Phys. Rev. Lett., 106, 181301, doi: [10.1103/PhysRevLett.106.181301](https://doi.org/10.1103/PhysRevLett.106.181301)
- Bartolo, N., et al. 2016, JCAP, 12, 026, doi: [10.1088/1475-7516/2016/12/026](https://doi.org/10.1088/1475-7516/2016/12/026)
- Baumann, D. 2011, in Theoretical Advanced Study Institute in Elementary Particle Physics: Physics of the Large and the Small, 523–686, doi: [10.1142/9789814327183_0010](https://doi.org/10.1142/9789814327183_0010)

³ Recent numerical and theoretical investigations imply that $\mathcal{R}_c \sim \mathcal{O}(1)$ (Musco et al. 2005, 2009; Nakama et al. 2014; Harada et al. 2013). Moreover, the proper value of the threshold depends on the shape of the power spectrum of the curvature perturbation. In this work, we consider $\mathcal{R}_c \sim 1.75$ according to the value of density threshold $\delta_c \sim 0.55$ quoted in (Musco et al. 2021b) by making use of the linear relation $\mathcal{R}_c = 9/(2\sqrt{2})\delta_c$ between curvature and density threshold (Drees & Erfani 2011; Young et al. 2014; Motohashi & Hu 2017).

- Baumann, D., Steinhardt, P. J., Takahashi, K., & Ichiki, K. 2007, *Phys. Rev. D*, 76, 084019, doi: [10.1103/PhysRevD.76.084019](https://doi.org/10.1103/PhysRevD.76.084019)
- Bhaumik, N., Ghoshal, A., & Lewicki, M. 2022, *JHEP*, 07, 130, doi: [10.1007/JHEP07\(2022\)130](https://doi.org/10.1007/JHEP07(2022)130)
- Biagetti, M., De Luca, V., Franciolini, G., Kehagias, A., & Riotto, A. 2021, *Phys. Lett. B*, 820, 136602, doi: [10.1016/j.physletb.2021.136602](https://doi.org/10.1016/j.physletb.2021.136602)
- Bird, S., Cholis, I., Muñoz, J. B., et al. 2016, *Phys. Rev. Lett.*, 116, 201301, doi: [10.1103/PhysRevLett.116.201301](https://doi.org/10.1103/PhysRevLett.116.201301)
- Braglia, M., Hazra, D. K., Finelli, F., et al. 2020a, *JCAP*, 08, 001, doi: [10.1088/1475-7516/2020/08/001](https://doi.org/10.1088/1475-7516/2020/08/001)
- Braglia, M., Hazra, D. K., Sriramkumar, L., & Finelli, F. 2020b, *JCAP*, 08, 025, doi: [10.1088/1475-7516/2020/08/025](https://doi.org/10.1088/1475-7516/2020/08/025)
- Bugaev, E., & Klimai, P. 2014, *Phys. Rev. D*, 90, 103501, doi: [10.1103/PhysRevD.90.103501](https://doi.org/10.1103/PhysRevD.90.103501)
- Byrnes, C. T., & Cole, P. S. 2021. <https://arxiv.org/abs/2112.05716>
- Byrnes, C. T., Copeland, E. J., & Green, A. M. 2012, *Phys. Rev. D*, 86, 043512, doi: [10.1103/PhysRevD.86.043512](https://doi.org/10.1103/PhysRevD.86.043512)
- Cai, R.-g., Pi, S., & Sasaki, M. 2019a, *Phys. Rev. Lett.*, 122, 201101, doi: [10.1103/PhysRevLett.122.201101](https://doi.org/10.1103/PhysRevLett.122.201101)
- Cai, R.-G., Pi, S., Wang, S.-J., & Yang, X.-Y. 2019b, *JCAP*, 05, 013, doi: [10.1088/1475-7516/2019/05/013](https://doi.org/10.1088/1475-7516/2019/05/013)
- Caravano, A., Komatsu, E., Lozanov, K. D., & Weller, J. 2022. <https://arxiv.org/abs/2204.12874>
- Carilli, C. L., & Rawlings, S. 2004, *New Astron. Rev.*, 48, 979, doi: [10.1016/j.newar.2004.09.001](https://doi.org/10.1016/j.newar.2004.09.001)
- Carr, B., Kohri, K., Sendouda, Y., & Yokoyama, J. 2021, *Rept. Prog. Phys.*, 84, 116902, doi: [10.1088/1361-6633/ac1e31](https://doi.org/10.1088/1361-6633/ac1e31)
- Carr, B., & Kuhnel, F. 2020, *Ann. Rev. Nucl. Part. Sci.*, 70, 355, doi: [10.1146/annurev-nucl-050520-125911](https://doi.org/10.1146/annurev-nucl-050520-125911)
- Carr, B., Kuhnel, F., & Sandstad, M. 2016, *Phys. Rev. D*, 94, 083504, doi: [10.1103/PhysRevD.94.083504](https://doi.org/10.1103/PhysRevD.94.083504)
- Carr, B. J. 1975a, *The Primordial black hole mass spectrum* —. 1975b, *Astrophys. J.*, 201, 1, doi: [10.1086/153853](https://doi.org/10.1086/153853)
- Carr, B. J., Kohri, K., Sendouda, Y., & Yokoyama, J. 2010, *Phys. Rev. D*, 81, 104019, doi: [10.1103/PhysRevD.81.104019](https://doi.org/10.1103/PhysRevD.81.104019)
- Cheng, S.-L., Lee, W., & Ng, K.-W. 2016, *Phys. Rev. D*, 93, 063510, doi: [10.1103/PhysRevD.93.063510](https://doi.org/10.1103/PhysRevD.93.063510)
- Clesse, S., & García-Bellido, J. 2017, *Phys. Dark Univ.*, 15, 142, doi: [10.1016/j.dark.2016.10.002](https://doi.org/10.1016/j.dark.2016.10.002)
- Corbin, V., & Cornish, N. J. 2006, *Class. Quant. Grav.*, 23, 2435, doi: [10.1088/0264-9381/23/7/014](https://doi.org/10.1088/0264-9381/23/7/014)
- Crowder, J., & Cornish, N. J. 2005, *Phys. Rev. D*, 72, 083005, doi: [10.1103/PhysRevD.72.083005](https://doi.org/10.1103/PhysRevD.72.083005)
- D’Amico, G., Kaloper, N., & Westphal, A. 2021, *Phys. Rev. D*, 104, L081302, doi: [10.1103/PhysRevD.104.L081302](https://doi.org/10.1103/PhysRevD.104.L081302)
- . 2022, *Phys. Rev. D*, 105, 103527, doi: [10.1103/PhysRevD.105.103527](https://doi.org/10.1103/PhysRevD.105.103527)
- Dimastrogiovanni, E., Fasiello, M., Hardwick, R. J., et al. 2018, *JCAP*, 11, 029, doi: [10.1088/1475-7516/2018/11/029](https://doi.org/10.1088/1475-7516/2018/11/029)
- Dimopoulos, S., Kachru, S., McGreevy, J., & Wacker, J. G. 2008, *JCAP*, 08, 003, doi: [10.1088/1475-7516/2008/08/003](https://doi.org/10.1088/1475-7516/2008/08/003)
- Domcke, V., Guidetti, V., Welling, Y., & Westphal, A. 2020, *JCAP*, 09, 009, doi: [10.1088/1475-7516/2020/09/009](https://doi.org/10.1088/1475-7516/2020/09/009)
- Domènech, G. 2021, *Universe*, 7, 398, doi: [10.3390/universe7110398](https://doi.org/10.3390/universe7110398)
- Domènech, G., Pi, S., & Sasaki, M. 2020, *JCAP*, 08, 017, doi: [10.1088/1475-7516/2020/08/017](https://doi.org/10.1088/1475-7516/2020/08/017)
- Drees, M., & Erfani, E. 2011, *Journal of Cosmology and Astroparticle Physics*, 2011, 005
- Durrer, R., Hollenstein, L., & Jain, R. K. 2011, *JCAP*, 03, 037, doi: [10.1088/1475-7516/2011/03/037](https://doi.org/10.1088/1475-7516/2011/03/037)
- Easther, R., & McAllister, L. 2006, *JCAP*, 05, 018, doi: [10.1088/1475-7516/2006/05/018](https://doi.org/10.1088/1475-7516/2006/05/018)
- Espinosa, J. R., Racco, D., & Riotto, A. 2018, *JCAP*, 09, 012, doi: [10.1088/1475-7516/2018/09/012](https://doi.org/10.1088/1475-7516/2018/09/012)
- García-Bellido, J., Peloso, M., & Unal, C. 2016, *JCAP*, 12, 031, doi: [10.1088/1475-7516/2016/12/031](https://doi.org/10.1088/1475-7516/2016/12/031)
- Green, A. M., & Kavanagh, B. J. 2021, *J. Phys. G*, 48, 043001, doi: [10.1088/1361-6471/abc534](https://doi.org/10.1088/1361-6471/abc534)
- Harada, T., Yoo, C.-M., & Kohri, K. 2013, *Physical Review D*, 88, 084051
- Inomata, K., Kawasaki, M., Mukaida, K., Tada, Y., & Yanagida, T. T. 2017, *Phys. Rev. D*, 95, 123510, doi: [10.1103/PhysRevD.95.123510](https://doi.org/10.1103/PhysRevD.95.123510)
- Janssen, G., et al. 2015, *PoS, AASKA14*, 037, doi: [10.22323/1.215.0037](https://doi.org/10.22323/1.215.0037)
- Kalosh, R., & Linde, A. 2022a, *JCAP*, 04, 017, doi: [10.1088/1475-7516/2022/04/017](https://doi.org/10.1088/1475-7516/2022/04/017)
- . 2022b. <https://arxiv.org/abs/2203.10437>
- Kalosh, R., Linde, A., & Yamada, Y. 2019, *JHEP*, 01, 008, doi: [10.1007/JHEP01\(2019\)008](https://doi.org/10.1007/JHEP01(2019)008)
- Kavanagh, B. J. 2019, *bradkav/PBHbounds: Release version, 1.0*, Zenodo, doi: [10.5281/zenodo.3538999](https://doi.org/10.5281/zenodo.3538999)
- Khlopov, M. Y. 2010, *Res. Astron. Astrophys.*, 10, 495, doi: [10.1088/1674-4527/10/6/001](https://doi.org/10.1088/1674-4527/10/6/001)
- Kohri, K., & Terada, T. 2018, *Phys. Rev. D*, 97, 123532, doi: [10.1103/PhysRevD.97.123532](https://doi.org/10.1103/PhysRevD.97.123532)
- Linde, A., Mooij, S., & Pajer, E. 2013, *Phys. Rev. D*, 87, 103506, doi: [10.1103/PhysRevD.87.103506](https://doi.org/10.1103/PhysRevD.87.103506)

- Linde, A., Wang, D.-G., Welling, Y., Yamada, Y., & Achúcarro, A. 2018, JCAP, 07, 035, doi: [10.1088/1475-7516/2018/07/035](https://doi.org/10.1088/1475-7516/2018/07/035)
- Lyth, D. H. 2012, JCAP, 05, 022, doi: [10.1088/1475-7516/2012/05/022](https://doi.org/10.1088/1475-7516/2012/05/022)
- Manchester, R. N., et al. 2013, Publ. Astron. Soc. Austral., 30, 17, doi: [10.1017/pasa.2012.017](https://doi.org/10.1017/pasa.2012.017)
- Matarrese, S., Mollerach, S., & Bruni, M. 1998, Phys. Rev. D, 58, 043504, doi: [10.1103/PhysRevD.58.043504](https://doi.org/10.1103/PhysRevD.58.043504)
- Matarrese, S., Pantano, O., & Saez, D. 1993, Phys. Rev. D, 47, 1311, doi: [10.1103/PhysRevD.47.1311](https://doi.org/10.1103/PhysRevD.47.1311)
- . 1994, Phys. Rev. Lett., 72, 320, doi: [10.1103/PhysRevLett.72.320](https://doi.org/10.1103/PhysRevLett.72.320)
- McAllister, L., Silverstein, E., & Westphal, A. 2010, Phys. Rev. D, 82, 046003, doi: [10.1103/PhysRevD.82.046003](https://doi.org/10.1103/PhysRevD.82.046003)
- Motohashi, H., & Hu, W. 2017, Physical Review D, 96, 063503
- Musco, I. 2019, Phys. Rev. D, 100, 123524, doi: [10.1103/PhysRevD.100.123524](https://doi.org/10.1103/PhysRevD.100.123524)
- Musco, I., De Luca, V., Franciolini, G., & Riotto, A. 2021a, Phys. Rev. D, 103, 063538, doi: [10.1103/PhysRevD.103.063538](https://doi.org/10.1103/PhysRevD.103.063538)
- . 2021b, Physical Review D, 103, 063538
- Musco, I., Miller, J. C., & Polnarev, A. G. 2009, Classical and Quantum Gravity, 26, 235001
- Musco, I., Miller, J. C., & Rezzolla, L. 2005, Classical and Quantum Gravity, 22, 1405
- Nakama, T., Harada, T., Polnarev, A., & Yokoyama, J. 2014, Journal of Cosmology and Astroparticle Physics, 2014, 037
- Namba, R., Peloso, M., Shiraishi, M., Sorbo, L., & Unal, C. 2016, JCAP, 01, 041, doi: [10.1088/1475-7516/2016/01/041](https://doi.org/10.1088/1475-7516/2016/01/041)
- Özsoy, O. 2018, JCAP, 04, 062, doi: [10.1088/1475-7516/2018/04/062](https://doi.org/10.1088/1475-7516/2018/04/062)
- . 2021, JCAP, 04, 040, doi: [10.1088/1475-7516/2021/04/040](https://doi.org/10.1088/1475-7516/2021/04/040)
- Özsoy, O., & Lalak, Z. 2021, JCAP, 01, 040, doi: [10.1088/1475-7516/2021/01/040](https://doi.org/10.1088/1475-7516/2021/01/040)
- Peloso, M., & Sorbo, L. 2022, <https://arxiv.org/abs/2209.08131>
- Pi, S., & Sasaki, M. 2020, JCAP, 09, 037, doi: [10.1088/1475-7516/2020/09/037](https://doi.org/10.1088/1475-7516/2020/09/037)
- Press, W. H., & Schechter, P. 1974, Astrophys. J., 187, 425, doi: [10.1086/152650](https://doi.org/10.1086/152650)
- Sasaki, M., Suyama, T., Tanaka, T., & Yokoyama, S. 2016, Phys. Rev. Lett., 117, 061101, doi: [10.1103/PhysRevLett.117.061101](https://doi.org/10.1103/PhysRevLett.117.061101)
- . 2018, Class. Quant. Grav., 35, 063001, doi: [10.1088/1361-6382/aaa7b4](https://doi.org/10.1088/1361-6382/aaa7b4)
- Schmitz, K. 2020, New Sensitivity Curves for Gravitational-Wave Experiments, v1, Zenodo, doi: [10.5281/zenodo.3689582](https://doi.org/10.5281/zenodo.3689582)
- . 2021, JHEP, 01, 097, doi: [10.1007/JHEP01\(2021\)097](https://doi.org/10.1007/JHEP01(2021)097)
- Shannon, R. M., et al. 2015, Science, 349, 1522, doi: [10.1126/science.aab1910](https://doi.org/10.1126/science.aab1910)
- Sorbo, L. 2011, JCAP, 06, 003, doi: [10.1088/1475-7516/2011/06/003](https://doi.org/10.1088/1475-7516/2011/06/003)
- Talebian, A., Nassiri-Rad, A., & Firouzjahi, H. 2022, Phys. Rev. D, 105, 103516, doi: [10.1103/PhysRevD.105.103516](https://doi.org/10.1103/PhysRevD.105.103516)
- Tomita, K. 1967, Progress of Theoretical Physics, 37, 831, doi: [10.1143/PTP.37.831](https://doi.org/10.1143/PTP.37.831)
- Wands, D. 2008, Lect. Notes Phys., 738, 275, doi: [10.1007/978-3-540-74353-8_8](https://doi.org/10.1007/978-3-540-74353-8_8)
- Weinberg, S. 2008, Cosmology
- Weltman, A., et al. 2020, Publ. Astron. Soc. Austral., 37, e002, doi: [10.1017/pasa.2019.42](https://doi.org/10.1017/pasa.2019.42)
- Wenren, D. 2014. <https://arxiv.org/abs/1405.1411>
- Yokoyama, S., Suyama, T., & Tanaka, T. 2008, Phys. Rev. D, 77, 083511, doi: [10.1103/PhysRevD.77.083511](https://doi.org/10.1103/PhysRevD.77.083511)
- Yoo, C.-M., Harada, T., Garriga, J., & Kohri, K. 2018, Progress of Theoretical and Experimental Physics, 2018, 123E01
- Young, S., Byrnes, C. T., & Sasaki, M. 2014, Journal of Cosmology and Astroparticle Physics, 2014, 045
- Young, S., Musco, I., & Byrnes, C. T. 2019, Journal of Cosmology and Astroparticle Physics, 2019, 012
- Zhou, Z., Jiang, J., Cai, Y.-F., Sasaki, M., & Pi, S. 2020, Phys. Rev. D, 102, 103527, doi: [10.1103/PhysRevD.102.103527](https://doi.org/10.1103/PhysRevD.102.103527)